

AD-A193 572

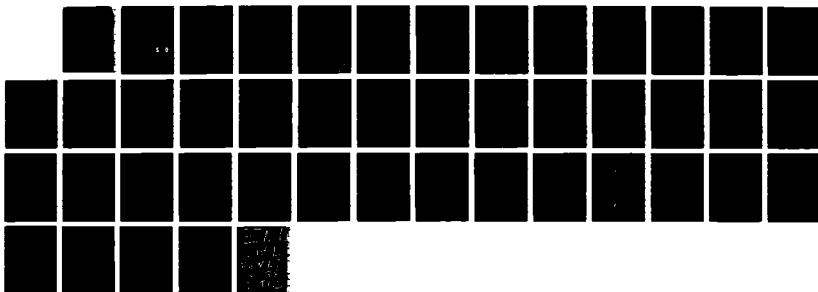
COLLOIDAL ASSEMBLIES EFFECT ON CHEMICAL REACTIONS(U)
TURIN UNIV (ITALY) E PELIZZETTI JUL 86
DAJA45-85-C-0023

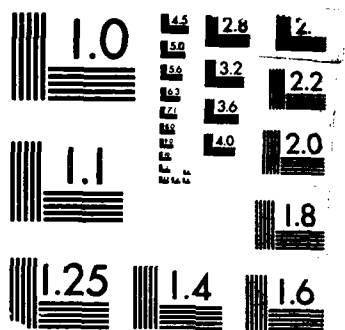
1/1

UNCLASSIFIED

F/G 7/3

NL





MICROCOPY RESOLUTION TEST CHART
 NBS 1963-A

AD-A193 572

COLLOIDAL ASSEMBLIES EFFECT ON CHEMICAL REACTIONS

E. Pelizzetti
Università di Torino
Contract n. DAJA 45-85-C-0023

DTIC FILE COPY

"Third Periodic Report"
February 1986 - July 1986

"The research reported in this document has been made possible through the support and sponsorship of the U.S. Government through its European Research Office of the U.S. Army. ~~This report is intended only for the internal management use of the Contractor and the U.S. Government.~~

DTIC
ELECTE
S APR 27 1988 D
H

DISTRIBUTION STATEMENT A

Approved for public release;
Distribution Unlimited

88 4 27 026

REPORT DOCUMENTATION PAGE		READ INSTRUCTIONS BEFORE COMPLETING FORM
1. REPORT NUMBER	2. GOVT ACCESSION NO.	3. RECIPIENT'S CATALOG NUMBER
4. TITLE (and Subtitle) COLLOIDAL ASSEMBLIES EFFECT ON CHEMICAL REACTIONS		5. TYPE OF REPORT & PERIOD COVERED FINAL AUGUST 1985 - AUGUST 1986
		6. PERFORMING ORG. REPORT NUMBER
7. AUTHOR(s) Ezio PELIZZETTI		8. CONTRACT OR GRANT NUMBER(s) DAJA 45-85-C-0023
9. PERFORMING ORGANIZATION NAME AND ADDRESS Università di Torino Via Verdi 8, Torino, Italy		10. PROGRAM ELEMENT, PROJECT, TASK AREA & WORK UNIT NUMBERS
11. CONTROLLING OFFICE NAME AND ADDRESS HQ. 47TH AREA SUPPORT GROUP P.O. BOX 160 WARRINGTON, CHESHIRE, ENGLAND		12. REPORT DATE SEPTEMBER 1986
14. MONITORING AGENCY NAME & ADDRESS (if different from Controlling Office)		13. NUMBER OF PAGES 21
		15. SECURITY CLASS. (of this report)
		15a. DECLASSIFICATION/DOWNGRADING SCHEDULE
16. DISTRIBUTION STATEMENT (of this Report)		
17. DISTRIBUTION STATEMENT (of the abstract entered in Block 20, if different from Report)		
18. SUPPLEMENTARY NOTES		
19. KEY WORDS (Continue on reverse side if necessary and identify by block number) COLLOIDS - MICELLES - MICROEMULSIONS - SURFACTANTS - OXIDATION - PHOTOCATALYSIS - DEGRADATION - HALOAROMATIC COMPOUNDS - REACTION MECHANISM - KINETICS		
20. ABSTRACT (Continue on reverse side if necessary and identify by block number) The influence that organized assemblies (micelles, microemulsions) and semiconductor colloids exhibits on chemical reactions has been investigated. In particular electron transfer reactions induced by light in the presence of semiconductor particles have been shown to completely degrade several haloaromatic compounds. .		

Phenol degradation has been investigated by carrying out experiments at different pH, phenol and TiO_2 content, oxygen partial pressure. Intermediate compounds (quinol and catechol) were detected and quantitative formation of CO_2 was assessed. Similarly, the photocatalytic degradation of 2,4,5-trichlorophenoxy acetic acid (2,4,5-T) and 2,4,5-trichlorophenol on TiO_2 led to complete mineralization into CO_2 and HCl . In the degradation of 2,4,5-T several intermediates were detected by GC-MS and a scheme for the photodegradation pathways was formulated. The applicability of this degradation process to other haloaromatic compounds was preliminarily assessed.

Since the proposed photodegradative mechanism involves the intervention of OH^\cdot radicals, Fenton's reagent ($\text{Fe}^{2+} + \text{H}_2\text{O}_2$) was investigated as possible reagent for halophenols degradation. The mineralization of these compounds was in fact found to occur and the effect of the concentration of Fe^{2+} , Fe^{3+} , HClO_4 was investigated.

Microemulsions are transparent dispersion of oil in water (O/W) or water in oil (W/O) in the presence of a surfactant and a cosurfactant. These aggregates can bring reactants together or to bring them apart and solubilize large amount of sparingly water soluble compounds.

The formation of the ground state charge transfer complex between durene and chloranil was investigated in O/W microemulsion. The effect of compartmentalization on the equilibrium constant was discussed and the equilibrium of formation or dissociation of the complex was found to occur in 1×10^{-3} s.

Electron transfer reactions between benzenediols and IrCl_6^{2-} was investigated over a wide range of microemulsion composition (from O/W to W/O). A three pseudo phase model accounting for the observed rate constants was proposed.

The complexing and extracting properties of a functionalized surfactant family (4-alkylamidosalicylic acids) were investigated. The acid-base properties of the surfactant ligands and the partitioning in the presence of non-ionic micelles were studied. The proper conditions for an efficient iron(III) complexation and extraction were determined.

Key words: oxidation, photocatalysis;
surfactants; reaction mechanism.

Progress of the research

The role of colloidal assemblies in the control of the mechanism and the rates of chemical reactions has been examined with particular interest for redox reactions. These reactions quite often represent in fact the first step of degradation process of organic compounds.

The electron transfer kinetics between benzenediols (catechols, and substituted catechols) and inorganic complexes, *e.g.* IrCl_6^{2-} has been investigated in the presence of O/W and W/O microemulsions (water, NaCl 1%/toluene/1-butanol/SDS). The rates of reactions are largely affected by microemulsion composition and concentration. The hydrophobicity of the substituents on the aromatic ring has also a relevant effect. A model for the understanding of these experimental results has been proposed. Additional informations on the effect of medium composition have been obtained by kinetic experiments in SDS/butanol and water/butanol mixtures.

The formation of the ground state charge transfer complex between durene and chloranil has been investigated in O/W microemulsion (CH_2Cl_2 /CTAB/butanol/water). The equilibrium of formation and dissociation of the complex is reached in less than one millisecond and the effect on the equilibrium constant is mainly due to a compartmentalization effect.

Recently, the degradation of a series of chlorophenols by means of H_2O_2 in the presence of Fe^{2+} has been investigated. We obtain complete mineralization, i.e. formation of CO_2 and HCl as final products; the acidity and $\text{Fe}^{3+}/2+$ contration markedly influence the rate of the process.

Semiconductor particles have been proved to be active photocatalyst in the degradation of organic compounds under solar light. A series of organic as well as haloaromatic compounds (chlorophenols, chlorobenzenes) has been examined and, in the presence of water and oxygen, the process gives rise to the formation of CO_2 and HCl as final products.

Detailed investigation of the mechanism of reaction for 2,4,5-T has been carried out by means of GC-MS.

For	
DTIC TAB	<input checked="" type="checkbox"/>
Unannounced	<input type="checkbox"/>
Justification	<input type="checkbox"/>
By <i>per form 50</i>	
Distribution/	
Availability Codes	
Dist	Avail and/or Special
A-1	



(2) RESEARCH PLANS

- Photodegradation of organic compounds by visible light. Other haloaromatic compounds, such as PCB and Dioxins, will be considered. Particular attention will be devoted in the investigation of the details of the reaction mechanism (adsorption-desorption process, kinetics, inhibition, nature of the semiconductor and its surface, detection of intermediates).

- The kinetics and mechanism of oxidation of organic compounds in the presence of organized assemblies, such as micelles and microemulsions, will be explored with particular attention to catalytic processes. In this light also complexation reactions of metal ions with functionalized surfactants will be investigated.

- The effect of solvent composition on electron transfer reactions will be examined.

- The physico-chemical properties of colloidal aggregates will be investigated, with particular attention to functionalized surfactants.

(3) No significative administrative actions occurred during the period reported.

(4) -----

(5) -----

(6) The funds of the first instalment are now available.

LIST OF PUBLICATIONS

- 1) V.Augugliaro, L.Palmisano, A.Sclafani, C.Minero, and E.Pelizzetti, "Photocatalytic Degradation of Phenol in Aqueous Titanium Dioxide Dispersions", submitted.
- 2) M.Barbeni, M.Morello, E.Pramauro, E.Pelizzetti, M.Vincenti, E.Borgarello, and N.Serpone, "Sunlight Photodegradation of 2,4,5-Trichlorophenoxyacetic acid and 2,4,5-Trichlorophenol on TiO_2 . Identification of Intermediates and Degradation Pathway", submitted.
- 3) M.Barbeni, C.Minero, E.Pelizzetti, E.Borgarello, and N.Serpone, "Chemical Degradation of Chlorophenols with Fenton's Reagent", submitted.
- 4) P.P.Infelta, R.Graglia, C.Minero, and E.Pelizzetti, "Ground State Charge Transfer Complexes in O/W Microemulsions", in "Surfactants and Colloids. Fundamentals and Applications", E.Barni and E.Pelizzetti eds., Ann.Chim., Soc. Chim. Ital., Rome, in press.
- 5) C.Minero, E.Pelizzetti and E.Pramauro, "Electron Transfer Reactions in Microemulsions", submitted
- 6) E.Pramauro, C.Minero and E.Pelizzetti, "Use of Amphiphilic Ligands in Chemical Separations", in "Use of Ordered Media in Chemical Separations", W.L.Hinze and D.W.Armstrong eds., ACS Symp. Ser., in press.

AD

COLLOIDAL ASSEMBLIES EFFECT ON CHEMICAL REACTIONS

~~Final~~ ^{THIRD} ~~Report~~ Report

by

Ezio PELIZZETTI

September 1986

United States Army
EUROPEAN RESEARCH OFFICE OF THE U.S. ARMY
London England

CONTRACT NUMBER DAJA 45-85-C-0023

Università di Torino, Italy

Approved for Public Release; distribution unlimited

Participating scientific personel

Edmondo PRAMAURO Associate Professor

Claudio MINERO Associate Researcher

LIST OF PUBLICATIONS

- 1) V.Augugliaro, L.Palmisano, A.Sclafani, C.Minero, and E.Pelizzetti, "Photocatalytic Degradation of Phenol in Aqueous Titanium Dioxide Dispersions", submitted.
- 2) M.Barbeni, M.Morello, E.Pramauro, E.Pelizzetti, M.Vincenti, E.Borgarello, and N.Serpone, "Sunlight Photodegradation of 2,4,5-Trichlorophenoxyacetic acid and 2,4,5-Trichlorophenol on TiO_2 . Identification of Intermediates and Degradation Pathway", submitted.
- 3) M.Barbeni, C.Minero, E.Pelizzetti, E.Borgarello, and N.Serpone, "Chemical Degradation of Chlorophenols with Fenton's Reagent", submitted.
- 4) P.P.Infelta, R.Graglia, C.Minero, and E.Pelizzetti, "Ground State Charge Transfer Complexes in O/W Microemulsions", in "Surfactants and Colloids. Fundamentals and Applications", E.Barni and E.Pelizzetti eds., Ann.Chim., Soc. Chim. Ital., Rome, in press.
- 5) C.Minero, E.Pelizzetti and E.Pramauro, "Electron Transfer Reactions in Microemulsions", submitted
- 6) E.Pramauro, C.Minero and E.Pelizzetti, "Use of Amphiphilic Ligands in Chemical Separations", in "Use of Ordered Media in Chemical Separations", W.L.Hinze and D.W.Armstrong eds., ACS Symp. Ser., in press.

CONTENT

I. Photodegradation of aromatic compounds by visible light	p. 1
- Phenol	
- 2,4,5-Trichlorophenoxyacetic acid	
- Other chlorinated compounds. Comments	
II. Oxidative degradation of organic compounds	p. 8
III. Chemical reactions in microemulsions	p.13
- Kinetics of ground state complex formation	
- Redox reactions in microemulsions	
IV. Characterization and properties of functionalized surfactants	p.19
- Extraction and complexing properties of hydrophobic salycilic acids	

Illustrations, Tables

Figure 1 - 11

Table 1 - 3

I. PHOTODEGRADATION OF ORGANIC COMPOUNDS BY VISIBLE LIGHT

Semiconductor particles have been proved to be active catalysts in organic transformations induced by light. Since Chloroaromatic derivatives are compounds of relevant concern because some of them are bioaccumulative and persistent in the environment and also extremely toxic, their behavior under solar light has been investigated. In fact microbial degradation and naturally occurring hydrolysis require long periods; direct photodegradation requires high energy photons often leading to incomplete decomposition and, in some cases, to the formation of dangerous products.

Heterogeneous photo-assisted catalytic degradation by means of semiconductor particles has been applied to a variety of aromatic compounds.

The efficiency of these photocatalyzed reactions depends on many factors and mainly on the nature of the semiconductor. Figure 1 shows the results of light exposure of aerated aqueous solutions of 3,4 dichlorophenol in the presence of 2 g/l of various semiconductor suspension, at constant pH and temperature. The spectral distribution of irradiation (from a Solarbox lamp) in the experimental range 310-830 nm corresponded to AM1 solar illumination. The experiments concerning phenol and 3,4,5-trichlorophenoxyacetic acid degradation were carried out mainly with TiO_2 as photocatalyst.

I.1. Phenol

A typical experiment of phenol photocatalytic degradation is reported in Figure 2 where also the intermediate benzenediol (quinol and catechol, identified by LC) concentration is shown.

The salient features experimentally observed can be summarized as follows:

- the photodegradation is pH dependent and the highest photo reactivity is observed in the alkaline region;
- there is not degradation in absence of oxygen;
- the presence of massive amount of Cl^- negatively affects the degradation rate;
- the degradation rate is negatively affected by the initial phenol concentration;
- the reflectance spectrum of TiO_2 is not affected by the phenol adsorbed from a solution at pH 3, whilst it is affected when the phenol is adsorbed from a solution at pH 13, anatase being more photoactive than rutile;

- intermediate compounds are detected which are unstable and photodegraded.

An indication of the catalytic nature is obtained from the sunlight experiments, for which it was observed that the reaction proceeded for months without showing any decline. Moreover a rough calculation of the turnover number, molecules converted/(sites·h), gives a figure of about 200, showing that the surface sites are renewed 200 times in one hour. This calculation was made considering an initial rate of phenol photodegradation of $60 \text{ mg l}^{-1} \text{ h}^{-1}$, $5 \cdot 10^{14}$ surface OH^- sites/ cm^2 and that for the complete phenol oxidation 28 electrons are required.

It may be safely assumed that in the alkaline slurry the surface of TiO_2 is fully covered with water molecules and with OH^- groups; in a somewhat similar situation it has been demonstrated that OH^- groups and water molecules are roughly in a 1:1 ratio. The OH^- groups will likely exhibit a range of acid-base strength, according to the nature of the sites in which they are accommodated.

As far as the rate determining step of the process is concerned, it can be excluded any influence of mass transfer rate limitation to the solid-liquid interface. It would arise if the phenol and oxygen concentrations on the TiO_2 surface were practically zero. By calculating the ratio between the maximum mass transfer rate and the reaction rate, it comes out to be of the order of magnitude of 10^3 . This consideration indicates that the slow step in the phenol photodegradation process concerns the surface catalytic reaction because the liquid-solid mass transfer rate offers a negligible resistance.

We may therefore state that the photodegradation reaction occurs between the reactants both adsorbed on the TiO_2 surface. These adsorbed species as well as others present on the surface like OH^- will be involved in the reaction. Therefore the extent and the rate of the reaction is affected by the nature of the interaction between the reactants with the surface as well as by the electronic properties of the irradiated semiconductor.

The reflectance spectra of TiO_2 on whose surface phenol from a pH 13 solution, i.e. phenate ion, is adsorbed, clearly indicate that this species interacts with the surface forming a complex able to absorb visible radiation, while the phenate ions solution is photoactive in the UV region of the spectrum only.

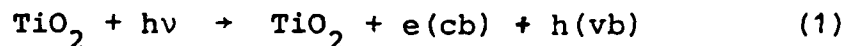
It is not straightforward to define how the phenate ions are bonded to a surface fully covered by water molecules and OH^- groups. We may only observe that the complex formed with the surface has an energy content higher than the ener

gy level of the phenate ion in solution and therefore it is prone to undergo a chemical transformation.

As for the oxygen, a variety of more or less stable species were detected according to the amount of hydroxylation, although there is a widespread agreement that the primary species in oxygen photoadsorption, in conditions similar to those used is O_2^- . Moreover it has been observed that oxygen photoadsorption is enhanced by the presence of hydroxyl groups while the presence of Cl^- groups, decreasing the OH^- content, decreases also the oxygen photoadsorption.

Having in mind the above considerations and also that, in absence of oxygen, no phenol photodegradation occurs, a tentative reaction scheme can be proposed.

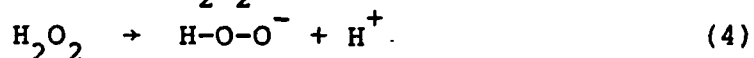
In a photocatalytic process the primary step is, of course, the photogeneration of pairs of electrons and holes which must be trapped to avoid recombination (charge separation):



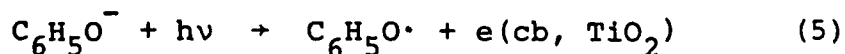
It is widely accepted that the hydroxyl groups are the likely traps for holes:



The possible destiny of $OH\cdot$ radicals can be described by the following reactions:

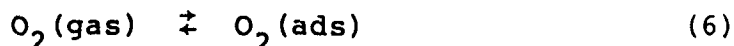


The peroxide ion is a well known oxidizing agent for organic substrates. In our case it must be also observed that, due to the fact that the surface phenate complex absorbs light at wavelength higher than that corresponding to the energy of the band gap of TiO_2 , the complex itself may act as sensitizer according the following reaction:

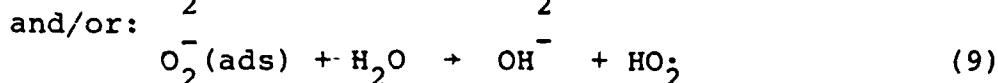
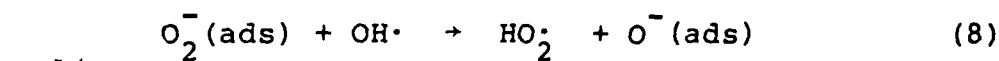


If this reaction takes place, then the phenate complex hastens the charge separation step and injects electrons to the conduction band of TiO_2 .

The traps for electrons are adsorbed oxygen species according to the following equations:

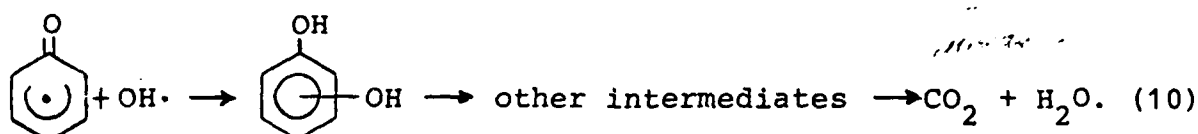


The superoxide species is unstable and reactive. It may evolve in several ways:

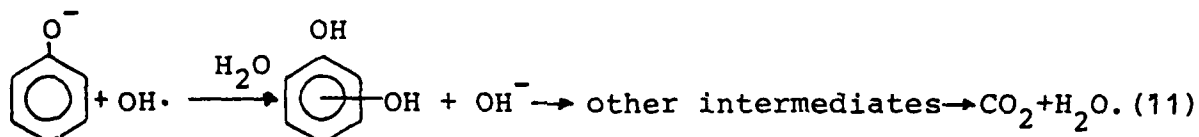


Thus as a consequence of the primary step of electrons and holes trapping, several species are produced, which will be involved in the reaction mechanism.

If the phenate ions act as sensitizer, thus forming radicals, these latter may likely evolve as follows:



In the phenate ion is still under an ionic form, the following scheme may be proposed:



The scheme proposed accounts for the main findings and indicates also the reasons why the photodegradation is lower in the acidic region. These reasons clearly are:

- the OH^- traps are much less in acidic medium than in the alkaline medium; therefore the charge separation step is less efficient;
- the reflectance spectra of TiO_2 , treated with phenol from acidic solution do not show appreciable change, indicating that the adsorption of phenol is very scarce;
- the chemisorption of O_2 in acidic medium is lowered with respect to the alkaline medium.

All these reasons affect in a negative way the course of the reaction in acidic medium. Finally it must be observed that adding Cl^- to the dispersions lowers the activity for the reasons already given. Of course this effect is much more evident in the acidic medium than in the alkaline medium where a very large amount of OH^- is present.

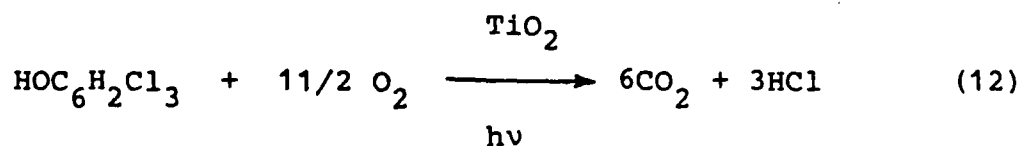
1.2. 2,4,5-Trichlorophenoxyacetic acid (2,4,5-7) and 2,4,5-Trichlorophenol (2,4,5-TCP)

As shown in Figure 1, chlorophenols can be photocatalytically degraded by semiconductor particles under visible light.

Because of its importance, the photocatalytic degradation

of 2,4,5-T has been investigated as well as that of 2,4,5-trichlorophenol which has been shown to be one of the major intermediate species.

Fig. 3a illustrates the complete degradation of 2,4,5-T and 2,4,5-TCP in aqueous suspensions of TiO_2 in the presence of air. Illumination ($\lambda \geq 340 \text{ nm}$) of $1 \times 10^{-4} \text{ M}$ of 2,4,5-T and 2,4,5-TCP in air and in the presence of suspended titanium dioxide results in the rapid disappearance of the chlorinated organic compounds with the concomitant formation of Cl^- (Fig. 3b). The amount of Cl^- (ca. $3 \times 10^{-4} \text{ M}$) and CO_2 formed confirms the complete mineralization of 2,4,5-T and 2,4,5-TCP. For example, 2×10^{-6} moles of 2,4,5-TCP gave 1.2×10^{-5} moles of CO_2 , according to the stoichiometric equation (12):

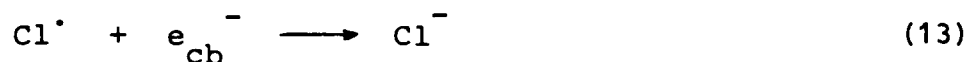


From the ratio between Cl^- formed and 2,4,5-T or 2,4,5-TCP degraded as a function of illumination time, it was observed that a difference exists between the degradation behaviour of the two chloro compounds; the ratio is 3 all along the reaction time for 2,4,5-TCP as expected from the stoichiometric decomposition (reaction 12). Such is not the case for the 2,4,5-T. In fact, only after 180 min of irradiation does the ratio between Cl^- formed and 2,4,5-T ($1 \times 10^{-4} \text{ M}$) consumed reach the value of 3, even though the total disappearance of 2,4,5-T from the solution occurs in less than 100 min (Figure 3).

According to these results, the degradation of 2,4,5-T, induced by irradiated TiO_2 dispersions, shows a very particular behaviour compared to the chlorophenols. In fact several intermediates were observed and identified by GC/MS after 20 min of irradiation under simulated AM1 conditions in aerated aqueous TiO_2 suspensions. The intermediate species were detected in a wide range of concentrations which showed to be crucial in proposing the several degradation pathways illustrated in Fig. 4. Of course, the identification of different intermediates is dependent on the stability of the intermediate itself as some of these species undergo further facile oxidation. As a consequence, observation and identification of trace quantities of an unstable intermediate product, as well as the high concentration of a very stable intermediate species contribute to the formulation of a plausible degradation mechanism. Trace amounts of different reaction products were analyzed by taking into account the contribution of the impurities present initial-

ly in 2,4,5-T as supplied by the vendor. Parallel analyses were carried out on the products from the treatment of the intermediate species with diazomethane in order to decrease their polarity and to better identify these products by mass spectrometric techniques.

2,4,5-TCP (III) and 2,4,5-trichlorophenyl formate (IV) are the two major and longer lived intermediate products of the photodegradation of 2,4,5-T. The OH^\bullet (and HO_2^\bullet) radicals generated through sequence (1)-(9) can subsequently undergo a series of reactions with the 2,4,5-T, leading to the products summarized in the scheme illustrated in Fig. 4. The details of the mechanism are not yet entirely clear; however, it seems plausible, by simple analogy with the photodegradation of 4-chlorophenol, that repeated hydroxyl attack on the aromatic ring will lead to chloride radicals and eventually also to some semiquinonoid type radicals. The Cl^\bullet radicals formed undergo subsequent reduction to Cl^- (reaction 13):



The semiquinone radicals formed can subsequently be oxidized (or can disproportionate), with the resulting benzoquinone undergoing further degradation via photocatalytic oxidation on TiO_2 as reported earlier. The photodegradation pathway reported in Fig. 4 is analogous to the mechanism proposed in the photochemical degradation of 2,4,5-T in the absence of TiO_2 , except that polymer formation was observed instead of complete mineralization to CO_2 and HCl when TiO_2 is present. It is worth noting that the simple process of dehalogenation appears not to be significant in the photocatalyzed degradation of 2,4,5-T reported here.

Finally, the activity of the TiO_2 Degussa P-25 powder was tested for the photodegradation of 2,4,5-T by performing several runs with the same TiO_2 powder: 1.5×10^{-4} M of 2,4,5-T was irradiated for 60 min leaving 1.1×10^{-5} M of non-decomposed substrate in solution. After this period, a fresh solution of 2,4,5-T was added and the photodegradation continued. This same cycle was repeated 11 times; the subsequent cycle was run for 120 min. At this point, the TiO_2 was washed with water, and then used again in the photodegradation process. From the results it is evident that the quantity of 2,4,5-T photodegraded with time is virtually constant and appears to have no consequence on the photo-activity of TiO_2 . This is taken to suggest that no adsorption of final products and no modification of the surface occur.

I.3. Other haloaromatic Compounds. Comments.

Since it was shown that TiO_2 exhibits the highest efficiency in the photodegradation of halophenols, it was chosen to investigate the decomposition of the series of chloroaromatic compounds listed in Table 1.

From these preliminary data it is evident that the process can be applied to a wide variety of compounds, even when present at very low concentrations. The observed degradation half-life ($t_{1/2}$) seems to be only slightly affected by the increase in the halogen content as well as by the solubility of the compound; experiments have also demonstrated that photodegradation proceeds at a significant rate also under direct sunlight.

For compounds which are scarcely soluble in water, such as DDT, 3,3'-DCB or 2,7-DCDD, the experiments were performed after stirring the substrate dissolved in n-hexane with the semiconductor. Upon evaporation of the solvent the catalyst was suspended in aqueous media and irradiated.

The adsorption-desorption properties of the organic compounds and other hazardous substrates, as well as detailed studies on the reaction mechanisms (including the detection of intermediate species) are in program.

Obviously the possibility of improving the rates and the efficiency of the processes through modification of the catalysts is actually actively pursued.

II. OXIDATIVE DEGRADATION OF ORGANIC COMPOUNDS

The degradation of organic pollutants by chemical oxidation affords an alternative route to the biological and natural routes, especially at high concentration of the contaminants. As shown in the previous section I the heterogeneous photocatalytic degradation of Chloro aromatic compounds proceeds through mechanism(s) in which $\text{OH}\cdot$ radical species may intervene in the reactions at irradiated aqueous slurries of TiO_2 .

Similarly, Fenton's reagent ($\text{Fe}^{2+} + \text{H}_2\text{O}_2$) easily induces the degradation of chlorinated phenols if excess H_2O_2 is used and O_2 is present in the reaction mixture.

Fig. 5 depicts the decrease in concentration of differently mono substituted chlorophenols as a function of time. The results demonstrate that the 3-chlorophenol (3-CP) is rapidly degraded in the presence of a $\text{Fe}^{2+}/\text{H}_2\text{O}_2/\text{O}_2$ mixture; disappearance of the analogous 2-CP and 4-CP is slower under the same conditions. Concomitant with the degradation of these CP species, an equimolar amount of free chloride ions in solution was detected (Fig. 5). A parallel experiment performed on the same reaction batch, but using HPLC techniques to detect the fate of the chlorophenols or its intermediates showed complete degradation of the aromatic ring. This implicates the occurrence of an oxidative process and not merely a simple dehalogenation substitution reaction. Analogous results were obtained for the dichlorophenols and trichlorophenols under identical conditions. In Table 2 are summarized the times necessary ($t/2$) to reduce the initial concentration of the chlorophenols in solution by a factor of two. It should be pointed out that this $t/2$ parameter is a practical operational parameter that includes any (if any) induction period to the start of the degradation reaction and must not be confused with the $t_{1/2}$ kinetic parameter for the reaction of disappearance. This procedure allows us to compare, in practical terms, the times required for the total degradation of these contaminants, even though the mechanism(s) may or may not be identical.

It is intriguing to note (cf. Fig. 5) that among the mono-chlorophenols, meta-chloro substitution induces a more rapid degradation than either of the ortho-chloro or para-chloro substitution. The differences in the rates of decomposition of these mono-chlorinated species is real. At higher $[\text{HClO}_4]$, the degradation is considerably inhibited as clearly noted in Table 2, which also summarizes $t/2$ values with changes in $[\text{HClO}_4]$. For the same HClO_4 concentration and for the same $\text{Fe}^{2+}/\text{H}_2\text{O}_2$ ratio, the 3,4-dichlorophenol (3,4-DCP) decomposes faster than any of the other compounds studied. In all cases, the stoichiometric quantity of free Cl^- was detected in solution at the completion of the reaction.

The formation of Cl^- is slower than the disappearance of the 3,4-DCP from the solution. Indeed, in a solution containing $3.0 \times 10^{-4}\text{M}$ of 3,4-DCP, $5.0 \times 10^{-5}\text{M}$ Fe^{2+} , $5.0 \times 10^{-3}\text{M}$ H_2O_2 and $5.0 \times 10^{-3}\text{M}$ of HClO_4 , the dichlorophenol disappears completely in < 25 min of reaction, while the expected stoichiometric amount of free Cl^- ($6.0 \times 10^{-4}\text{M}$) in solution for complete degradation of 3,4-DCP is obtained only after 250 min of reaction. This suggests that chloroaliphatic intermediate(s) may be formed after the opening of the benzene ring. This time lag between the disappearance of the phenol and the complete appearance of the product(s) (here, Cl^- ions) depends on the number of chloro substituents on the aromatic ring. For instance, for the mono-chloro derivatives, the disappearance of the chlorophenols and the appearance of stoichiometric amounts of chloride occur at nearly similar times (see Fig. 5). The results of Table 2 also indicate that a HClO_4 effect exists, and at higher concentrations of this acid the reaction is slower.

The disappearance of 3,4-DCP ($3.0 \times 10^{-4}\text{M}$) as a function of time, for three different concentrations of HClO_4 , is reported in Fig. 6; the other reagents were kept at $[\text{Fe}^{2+}] = 5.0 \times 10^{-5}\text{M}$, $[\text{H}_2\text{O}_2] = 5.0 \times 10^{-3}\text{M}$. Thus a tenfold increase of $[\text{HClO}_4]$, from $5.0 \times 10^{-3}\text{M}$ to $5.0 \times 10^{-2}\text{M}$, leads to an increase of $t/2$ from ~ 7 min to ~ 85 min. In the degradation of other chlorophenols, an increase of $[\text{HClO}_4]$ increases the induction period for the degradation process. A typical example is portrayed by the decomposition of 4-CP. Where $[\text{HClO}_4]$ is $1.5 \times 10^{-2}\text{M}$, no detectable degradation occurs for ~ 4 100 min. The $t/2$ is > 180 min (Table 2).

Another important parameter to consider was the effect of the Fe^{2+} concentration.

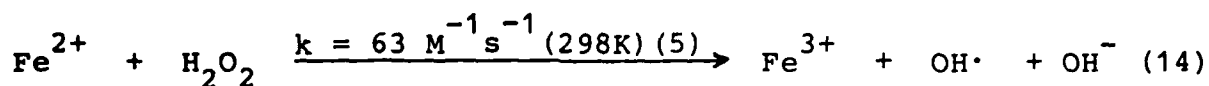
Increasing the $[\text{Fe}^{2+}]$ in solution for a fixed $[\text{H}_2\text{O}_2]$ at $5.0 \times 10^{-3}\text{M}$ increases the rate of decomposition. At concentration $> 2.0 \times 10^{-4}\text{M}$ in Fe^{2+} , the decomposition was too fast to follow with our techniques for reasonably reproducible results.

Finally the effect of Fe^{3+} on the degradation of 4-CP in a H_2O_2 /chlorophenol mixture was investigated. The reaction was carried out at 10^{-2}M in HClO_4 . Addition of Fe^{3+} (instead of Fe^{2+}) is inconsequential in the degradative process. However, an equivalent concentration of Fe^{2+} brings $t/2$ to ~ 50 min.

Equimolar amounts of Fe^{3+} and Fe^{2+} in the same reaction mixture increase the reaction rate ($t/2 \sim 20$ min). No doubt, Fe^{3+} is an important species in the complex degradative process.

The results herein reported may be interpreted on the basis of the following considerations. The interaction of iron(II) ions with hydrogen peroxide yields OH^\cdot radicals and iron(III)

(equation 14). The $\text{OH}\cdot$ formed, can easily



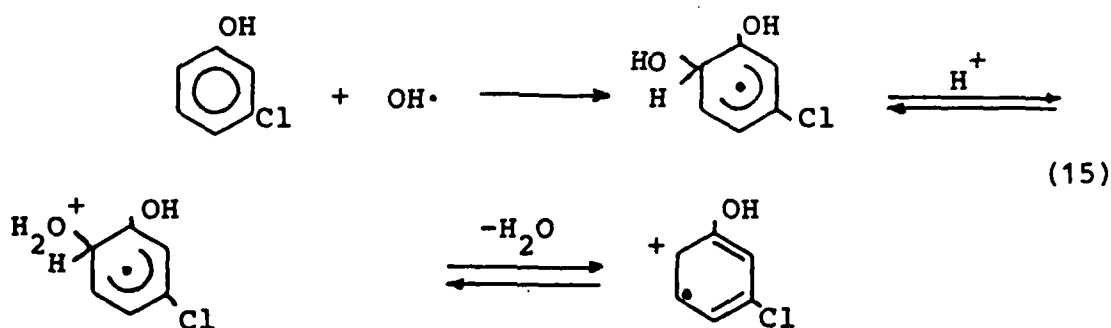
interact with an aromatic compound inasmuch as $\text{OH}\cdot$ radicals are good electrophiles.

In the presence of oxygen, oxidation of the intermediate species $(\text{HOClC}_6\text{H}_3\text{H}(\text{OH}))$ is preferred even if dimerization is still possible.

By analogy with earlier work on hydroxylations of aromatics, the degradative oxidation of chlorophenols probably proceeds via a hydroxylated species following which ring opening occurs to yield aldehydes and ultimately degradation ensues to CO_2 and Cl^- .

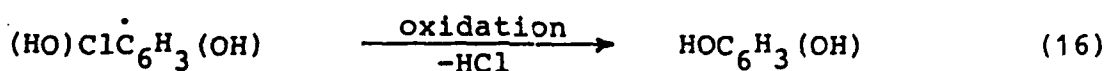
Various factors may contribute to the above experimental observations.

It can be tentatively suggested as a first step the formation of a radical cation by acid-catalyzed dehydration of the radical formed between the interaction of $\text{OH}\cdot$ with the chlorophenols (reaction 15). Evidences of the formation of radical-cations in acid media have been reported for methoxylated benzoic



acids. The different stabilities of the radical-cations formed for other chlorophenols may be an important factor responsible for the induction period observed in the degradation of chlorophenolic compounds at higher acidity. In fact, chlorine substituents in ortho and para positions can stabilize the positive charge of the radical-cation of eq. 15 better than meta-chlorine.

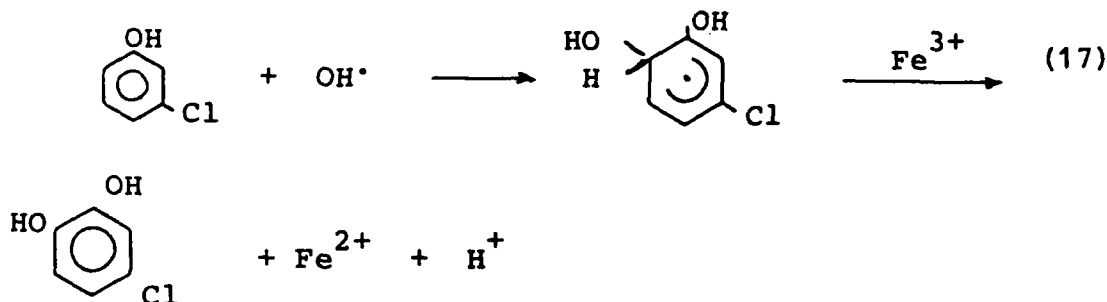
An alternative route of degradation is shown in eq. 16:



The formation of resorcinol as an intermediate product in the degradation reaction of 3-CP has been detected by HPLC technique.

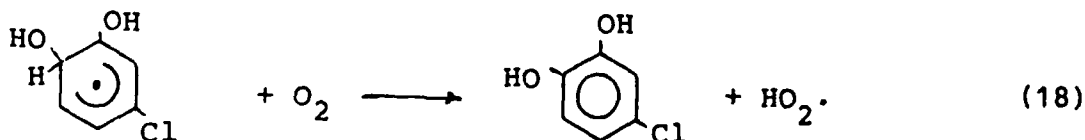
The increase in the oxidation rate of the decomposition of these chlorinated aromatic substrates when the amount of Fe^{2+} is increased from $3.0 \times 10^{-5}\text{M}$ to $2.0 \times 10^{-4}\text{M}$ is the result of an increase in the concentration of $\text{OH}\cdot$ produced according to reaction 14. Under our experimental conditions, it was not possible to investigate the process at higher $[\text{Fe}^{2+}]$ as the reaction was too rapid, even at higher $[\text{HClO}_4]$.

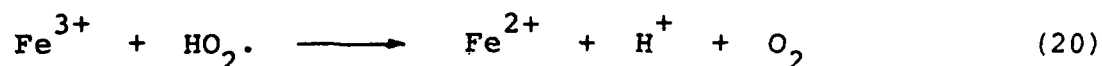
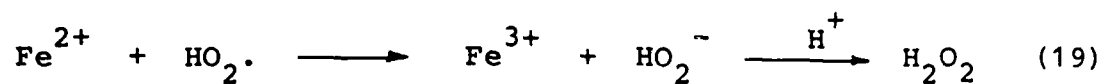
Iron(III) alone with H_2O_2 has very little effect, if any, on the degradation reaction (no $\text{OH}\cdot$ radicals can be formed). However, inasmuch as $\text{HO}_2\cdot$ radicals form from $\text{Fe}^{3+}/\text{H}_2\text{O}_2$ mixtures, these are inconsequential in the first step of the decomposition. Equivalent amounts of Fe^{2+} and Fe^{3+} increase the rate of oxidation more than the presence of Fe^{2+} alone. Furthermore, in a typical experiment (cf. Table 2), the amount of Fe^{2+} is catalytic compared to H_2O_2 and chlorophenol concentrations. Since reaction 14 is stoichiometric and almost complete degradations of the chlorophenols are obtained, reduction of Fe^{3+} to Fe^{2+} must occur. These considerations suggest the possible occurrence of reaction 17. That $\text{Fe}^{2+}/\text{Fe}^{3+}$ mixtures enhance the



degradation of the chlorophenols, while the presence of a large concentration of HClO_4 inhibits the reaction, is indicative of the competitiveness of reactions 15, 16 and 17.

Oxygen also has an effect on the hydroxylation reactions since it can act as a radical scavenger as noted in reaction 18. Following this, the $\text{HO}_2\cdot$ species can successively react with either Fe^{2+} or Fe^{3+} (reaction 19,20) to regenerate H_2O_2 and Fe^{2+} .





Further reaction of these hydroxylated aromatic species with the oxidizing agents in solution leads to the degradation products.

The disappearance of chlorophenols and appearance of free chloride in solution (Fig. 5) follow neither first nor second order kinetics, which appear to be quite complex. Further studies will address the nature of the various species in the hope of clarifying the pathway(s) of the degradation process.

Comments

These studies have shown that the utilization of Fenton's reagent affords an attractive possibility of decomposing chlorinated aromatic contaminants. Other studies, in program are directed at the potential degradation of pollutants and may contribute to the resolution of environmental problems such as the control and disposal of wastes.

III. CHEMICAL REACTIONS IN MICROEMULSIONS

Microemulsions are transparent dispersions of an oil in water (O/W) or water in oil (W/O) in the presence of a surfactant and a cosurfactant.

These dispersions form spontaneously upon mixing and contain spherical droplets, having usually diameters of 10-60 nm. The O/W microemulsions have similarities to normal micelles in water, and can be described as a stable collection of "oil" microdroplets in an aqueous continuous phase, while W/O microemulsions should be similar to the reverse micelles in apolar solvents.

The submicroscopic aggregates can bring reactants together or keep them apart, and can also exert a medium effect. As reaction media however the microemulsions can incorporate relatively large amount of solute and the volume of the disperse phase can generally be varied over a fairly wide range.

Whereas reactions in micelles have been studied extensively, processes in microemulsions (particularly electron transfers) have been scarcely examined.

Two model reactions (see below) have been investigated in order to obtain informations on the properties of microemulsions as reaction media.

III.1. Ground State Charge Transfer Complexes in O/W Microemulsions

Solute migration in microheterogeneous media still raises a number of questions as to its rates and mechanism.

In aqueous micellar solution, a number of investigations have led to a reasonable understanding of the solubilization of solutes as well as some of the mechanisms of their migration. For example, a dynamic exchange of CH_2I_2 takes place between bulk and sodium dodecylsulphate (10^{-1} M) micelles at a rate of the order of 10^7 s^{-1} . It is clear however that the rate of such processes is highly dependent upon the hydrophobic/hydrophilic character of the solute, as well as the nature of the microheterogeneous aggregates.

In order to clarify this point the formation of the ground state charge transfer complex between durene and chloranil was investigated in CH_2Cl_2 and in oil-in-water (O/W) microemulsions. The CH_2Cl_2 or CH_2Cl_2 /hexadecane microemulsion systems are stabilized by a cationic (hexadecyltrimethylammonium bromide) surfactant and 1-butanol as cosurfactant.

Since the equilibrium constant for the formation of charge transfer complex is 0.66 M^{-1} in CH_2Cl_2 and 8.4 M^{-1} in μE ,

it is evident that the compartmentalization introduced by the microemulsion structure favors drastically the CT complex formation.

If one writes the law of mass action with respect to the non-aqueous volume, one would expect to have

$$\frac{|DA|_0}{|D|_0 |A|_0} = K_H \quad (21)$$

where concentrations are measured with respect to the oil phase. This may be transformed to use average concentration (with respect to the total volume). One obtains

$$\frac{|DA|}{|D| |A|} = K_H \frac{V_t}{V_0} = K_M \quad (22)$$

where V_t is the total solution volume and V_0 is the "oil phase" volume. From the measured K_H and K_M one obtains that V_t/V_0 should be 12.6.

Under the assumption that there is no change in the density of water in the microemulsion systems, the ratios V_t/V_0 for the two microemulsions can be evaluated to be ca. 3, which does not account for the experimental ratio K_M/K_H . For the O/W systems considered here, the structure of the droplets may be described as a stable collection of "oil" microdroplets in an aqueous continuous phase. Each droplet consists of a "bulk" oil drop surrounded by a thick interphase consisting mainly of alcohol molecules and cationic surfactant. Then, if the ratio V_t/V_0 is calculated as $\Sigma(w_i/d_i) / \Sigma(w_0/d_0)$ (where d is the density, the subscript 0 refers to CH_2Cl_2 and hexadecane and i to all the components) values ranging from 7 to 10 can be estimated (depending on the microemulsion and on the assumptions concerning the density of the non-oil material).

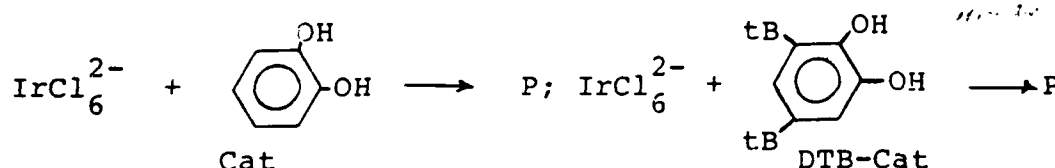
Thus, if the charge transfer complex is confined in CH_2Cl_2 or CH_2Cl_2 /hexadecane component, the change in the equilibrium constant from homogeneous to microemulsion medium should mainly be due to the decrease of the available volume for the solutes (A and D) in the microemulsion system. In this last hypothesis, the apparent lack of effect of the compartmentalization should be related to the solute (or complex) dynamic exchange between microemulsion droplets.

Using stopped-flow experiments, attempt was performed to measure the rate at which equilibrium is attained when mixing two identical microemulsions, one containing D and the other containing A, or one containing the charge transfer com

plex and the other only the microemulsion. Under all conditions, the expected equilibria were reached faster than the 1 millisecond time response of our equipment. Whatever the mechanisms involved we can say that equilibrium is obtained at a rate faster than $1 \times 10^3 \text{ s}^{-1}$.

III.2. Electron Transfer Reactions in μE

Degradation reactions often go through initial redox steps. As an example of electron transfer reaction involving organic substrates and oxidizing metal complexes in μE systems the following reactions have been selected:



- Pseudoternary phase diagram

The single-phase limits were experimentally determined (Fig. 7). By comparison with other phase diagrams reported for the same Butanol/SDS ratio, and from conductivity measurements (Fig. 8), it can be assumed that the microstructure changes from swollen micelles, through a bicontinuous phase, to reverse micelles. Whereas the lower phase limits can be explained by various current theories, the upper limit can be rationalized in terms of a failure of the bulk aqueous phase. The kinetic measurements were performed along the dilution lines, in which the Butanol/SDS/Toluene ratio was kept constant (see Fig. 7).

- Kinetic measurements

The variation of k_{exp} measured by stopped-flow as a function of the microemulsion composition is depicted in Fig. 9. For both investigated catechols, the following behavior has to be noted: - at higher water fractions inhibition is observed (which is more pronounced for DTB-Cat); - at lower water content there is an increase in reaction rates inversely dependent on the oil content.

- Three pseudophases model

A simple microemulsion model, consisting of three distinct pseudophases, without any assumptions about the microstructure, is proposed.

The following kinetic equation holds:

$$k_{\text{exp}}^{\mu\text{E}} = \chi_w \delta_w k_w \frac{\bar{C}_A(w) \bar{C}_B(w)}{\bar{C}_A(\text{Tot}) \bar{C}_B(\text{Tot})} + \chi_I \delta_I k_I \frac{\bar{C}_A(I) \bar{C}_B(I)}{\bar{C}_A(\text{Tot}) \bar{C}_B(\text{Tot})} + \chi_o \delta_o k_o \frac{\bar{C}_A(o) \bar{C}_B(o)}{\bar{C}_A(\text{Tot}) \bar{C}_B(\text{Tot})} \quad (23)$$

where: k is the second order rate constant in the micro-emulsion; δ 's are the densities of the microemulsion and of pseudophases; k 's are the specific rates constants in each phase; C 's are the local concentrations of the reagents expressed in moles/mass: x 's are the pseudophases molar fractions.

The partition coefficients for each reagent R ($A = \text{IrCl}_6^{2-}$, $B =$ catechols), are defined as follows: P_{WI}^A , P_{WI}^B , P_{WO}^A , P_{WO}^B , where:

$$P_{WF}^R = \exp\left(\frac{\mu_W^{OR} - \mu_F^{OR}}{RT}\right) = \frac{\chi_F^R \gamma_F^R}{\chi_W^R \gamma_W^R}$$

By substituting into equation (23):

$$k_{EXP} = \frac{\frac{k'_W}{\chi_W} + \frac{k'_I}{\chi_I} P_{WI}^A P_{WI}^B R_I^2 + \frac{k'_O}{\chi_O} P_{WO}^A P_{WO}^B R_O^2}{(1 + P_{WI}^A R_I + P_{WO}^A R_O)(1 + P_{WI}^B R_I + P_{WO}^B R_O)} \quad (24)$$

where $k' = k \cdot \delta$, $P_{WF}^R = P_{WF}^R \cdot \gamma_W^R / \gamma_F^R$, $R_I = (\sum_i n_i)_I / (\sum_i n_i)_W$; $R_O = (\sum_i n_i)_O / (\sum_i n_i)_W$.

In order to solve the equation (24), it is necessary to calculate the terms R_I and R_O .

Some assumptions about the composition of each pseudophase must be made:

$$(\sum_i n_i)_W = n_{W(W)} + n_{But(W)} \quad (25)$$

$$(\sum_i n_i)_I = n_{W(I)} + n_{But(I)} + n_{SDS(I)} + n_{Tol(I)} \quad (25)$$

$$(\sum_i n_i)_O = n_{But(O)} + n_{Tol(O)}$$

Thermodynamics imposes that the components present in each pseudophase must be in equilibrium. The eq. (24) and the appropriate mass balances can be solved in terms of mass transfer constants and activity coefficients. Since the system is far from ideality, another approach which takes in account the mutual solubility limits between the components, can be also proposed.

The moles of the components in each pseudophase can be related through proportionality constants α . It is assumed, in other words, that each pseudophase is always saturated with respect to the components present in defect. α 's coefficients are in fact solvation numbers.

$$\begin{aligned} n_{But(W)} &= \alpha_1 n_{W(W)} ; n_{W(I)} = \alpha_2 n_{SDS(I)} + \alpha_3 n_{BUT(I)} \\ n_{But(O)} &= \alpha_4 n_{Tol(W)} ; n_{Tol(I)} = \alpha_5 n_{SDS(I)} \end{aligned} \quad (26)$$

where α_1 represents the solubility of n-Butanol in water (0.017); α_2 is the hydration number for SDS in the inter-phase; α_3 is the solubility of water in n-Butanol (ca.1); α_4 is the solubility of n-Butanol in Toluene (); α_5 represents the average number of Toluene molecules per surfactant. It is obvious from these assumptions that the present model is not valid at the corners of the phase diagram.

- Analysis of the experimental data

The multiparametric kinetic equation was solved by computer simulation using eq. (24), (25), (26) with the following assumptions:

a) partition of microemulsion components. Since the solubilities of Butanol in water and Toluene are very low, $\alpha_1 = \alpha_4 = 0$. α_2 and α_3 are fitted by assuming that the upper demixing line is due to the failure of the aqueous pseudo-phase. The best fitting curves gave the following values: $\alpha_1 = \alpha_4 = 0$, $\alpha_2 = 3-3.5$, $\alpha_3 = 1$, and $\alpha_5 = 1$. The hydration number for SDS (α_2) is in agreement with the literature data.

b) partition of reagents. P_{WF}^{IR} is assumed to be constant. The estimated P_{WF}^{IR} values for catechols have to be consistent with the partition data obtained both from kinetic and HPLC measurements for SDS, whereas $P_{WF}^{IrCl_6^{2-}}$ must be very low.

c) kinetic parameters. k_W was measured as a function of dissolved Butanol. We used in the fitting the k_W value obtained in Butanol-saturated solution. k_I is a fitting parameter ($k_{But} < k_I < k_W$. k_{But} is the specific rate in the water-saturated Butanol solution). In eq. (24) the term depending on k_O was neglected.

On the basis of the above mentioned assumptions, the fitting parameters to be evaluated are: P_{WI}^B , P_{WD}^B , P_{WI}^A , k_I .

The obtained fitting curves are shown in Fig. 5. They were calculated using the following values:

	$k_W(\text{exp})$	k_I	$P_{WI}^{IrCl_6^{2-}}$	P_{WI}^{Cat}	P_{WO}^{Cat}
Cat	$3.9 \cdot 10^3$	$7.5 \cdot 10^3$	0.2	25	35
DTB-Cat	$7.0 \cdot 10^4$	$3.2 \cdot 10^4$	0.2	$5.0 \cdot 10^4$	$5.0 \cdot 10^5$

where $P_{WF}^{IR} = 55.5(K_B^R + \bar{v}_r)$; \bar{v}_r is the molar volume of the interphase; K_B^R is the usual binding constant (M^{-1}).

- Comments

The parameters evaluated using the model are in good agreement with those measured using independent techniques.

Although many simplifications have been introduced in the

model, the curve fitting is quite satisfactory.

The hypothesis of interphase hydration is crucial for explaining both the upper demixing line and the kinetic data.

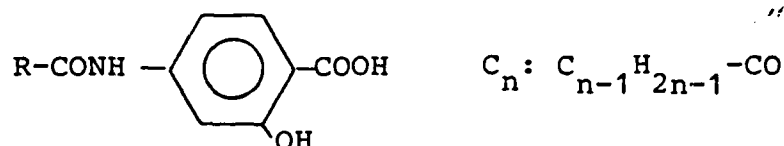
The microemulsion systems appear suitable media for carrying out redox reactions involving highly hydrophobic compounds and hydrophilic metal complexes.

IV. CHARACTERIZATION AND PROPERTIES OF FUNCTIONALIZED SURFACTANTS

Functionalized surfactants are amphiphilic molecules in which the polar head group can exhibit a chemical reactivities, such as complexing capability or electron transfer properties.

The complexing behavior could be used in chemical separations and in catalytic processes in organized assemblies.

As model system, the properties of a series of compounds containing the same chelating moiety, namely 4-aminosalicylic acid, with different alkyl chains, was investigated. The structure of the ligands (PAS-C_n) is the following:



Since aggregation occurs for these compounds only at high pH values, a study of complexing properties of aggregates in the presence of usual transition metal ions cannot be performed. At lower pH, however, the PAS-C_n molecules can be readily solubilized in the presence of nonionic surfactants (e.g. Brij 35: polyoxyethylene(23)dodecanol) and the obtained mixed micelles exhibit complexing capability in acidic media.

- Binding Constants of Ligands with Nonionic Micelles

The acid-base properties of the amphiphilic ligands change in the presence of micellar aggregates due to the well known partition equilibrium of both the acid and anionic form. A continuous increase in the apparent pK_a was observed with increasing concentration of micellized surfactant.

According to the simple pseudophase model of Berezin, the binding constants between the ligands and the micelles have been calculated using the following equation:

$$K_{a(\text{app})}^{-1} = K_{a(w)}^{-1} + K_{\text{HA}} \cdot K_{a(w)}^{-1} \cdot C_D \quad (27)$$

where K_{a(app)} is the dissociation constant of carboxylate group in the presence of Brij 35, K_{a(w)} is the same constant in water, K_{HA} is the binding constant of the undissociated PAS-C_n to the micelles and C_D is the concentration of micellized surfactant (C_D = C_{tot} - CMC). The critical micellar concentration for Brij 35, measured with the surface tension method is 6x10⁻⁵ M, in the experimental conditions.

For the investigated PAS-C_n ligands, the binding constant

for the undissociated form clearly increases with n , from 170 M^{-1} for C_2 and 500 M^{-1} for C_4 up to ca. 1500 M^{-1} for C_7 , whereas for the anionic form it becomes significant only for C_7 (110 M^{-1}). The obtained data is in good agreement with the values estimated from $\text{pK}_{\text{a}}(\text{app})$ shift, at low surfactant concentration, and allow us to define a minimum chain length for the ligand in order to have a strong binding to the micelles, both in acidic or anionic form.

- Complex Formation Constant in the Presence of Micelles
The kinetics and the complex formation equilibria in the presence of nonionic micelles have been also investigated, at constant acidity. The stoichiometry was assessed by using Job's method and the apparent stability constants were evaluated according to Frank and Ostwalt procedure, as previously reported for the system iron/salicylate in homogeneous aqueous solution.

For the equilibrium reaction:



where HSal^- indicates the dissociated chelating moiety of the ligand, the observed changes in the apparent formation constants (K_{C}) can be directly related with the variation of the apparent pK_{a} , previously discussed. In the conditions reported in the experimental section, the K_{C} values lie in the range $(2.5-4.0) \times 10^3$.

The experiments performed clearly showed that, whereas the complexation of iron(III) is not very much dependent on the ligand hydrophobicity, the association of the charged 1:1 chelates to the micelles and then the efficiency of the concentration process, markedly increases.

- Extraction of Iron(III) from Micellar Solutions

The surfactant system Triton X 100 / BL 4.2 was chosen because its suitable cloud temperature range and the good solubilizing capability towards the ligands.

The analyte content, after extraction, was determined both in the micellar and in the aqueous rich phase by VIS-spectrophotometry. Calibration curves were made with micellar phases containing the dissolved ligands, in the absence of iron (III). To these solutions, separated by centrifugation, were added known amounts of analyte and the absorbances were recorded.

The standard addition method was also applied to the extracted micellar layers containing iron(III). The results obtained with both procedures were in good agreement, as well as which obtained from DC-plasma spectrometry after analysis

of the aqueous dilute phases.

The extraction efficiency was then calculated from at least four independent measurements; the influence of the experimental parameters was also investigated.

Fig. 11 shows the effect of the ligand hydrophobicity on the analyte recovery, measured at pH 3.5, in the presence of Triton X100 (1% w/v) and BL 4,2 (1% w/v); added NaNO_3 : 5% w/v; iron(III): $1 \times 10^{-4} \text{ M}$ and PAS-C: $2 \times 10^{-3} \text{ M}$.

As it can be seen, quantitative recovery of iron(III) has been obtained in the reported conditions using the more hydrophobic compounds (PAS-C₁₀ or higher analogues). However, the lower solubility of these long chain molecules can limit the ligand concentration available in the system, keeping the volume of extraction micellar phase constant.

The extraction performances under different experimental conditions (i.e. varying the pH, the composition of surfactant mixtures, the amount of chelating compound) were also investigated for our test system. The results are shown in Table 3.

- Comments

The results obtained with the reported extraction model showed that the separation of charged species is possible, provided a suitable ligand hydrophobicity. Further developments of these multiphase extraction systems will require an accurate investigation of the equilibria and kinetic processes occurring at the interfaces, as well as the study of the micellar structure and properties of the host aggregates.

Other functionalized surfactants having various complexing groups and modular lipophilic chains, together with different nonionic solubilizing surfactants, are presently under investigation.

Table 1.- Half-lives for the Total Photodegradation of Contaminants Assisted by TiO_2 on Exposure to Simulated Sunlight^a.

COMPOUND	ABBREV.	CONCENTRATION (ppm)	pH	$t_{1/2}$ (min)
4-chlorophenol ^b	4-CP	6	3.0	14
3,4-dichlorophenol	3,4-DCP	18	3.0	45
2,4,5-trichlorophenol	2,4,5-TCP	20	3.0	55
Pentachlorophenol ^b	PCP	12	3.0	20
Sodium pentachlorophenate	NaPCP	12	10.5	15
Chlorobenzene	CB	45	2.5	90
1,2,4-trichlorobenzene	1,2,4-TCB	10	3.0	24
2,4,5-trichlorophenoxyacetic acid	2,4,5-T	32	3.0	40
4,4'-dichlorodiphenyltrichloroethane ^c	4,4'-DDT	1	3.0	46
3,3'-dichlorobiphenyl ^c	3,3'-DCB	1	3.0	10
2,7-dichlorodibenzo-p-dioxin ^c	2,7-DCDD	0.2	3.0	46

^a: Concentration of catalyst, 2.0 g/l; aerated aqueous solutions; wavelength >330 nm.

^b: Wavelength >310 nm.

^c: Adsorbed on TiO_2

TABLE 2 - Half-lives ($t/2$; see text) of Decomposition
of Various Chlorinated Phenols: $[\text{Fe}^{2+}] =$
 $5.0 \times 10^{-5} \text{ M}$, $[\text{H}_2\text{O}_2] = 5.0 \times 10^{-3} \text{ M}$,
 $[\text{chlorophenols}] = 3.0 \times 10^{-4} \text{ M}$.

Compound	$t/2$ at $5.0 \times 10^{-3} \text{ M}$ HClO_4 (min)	$t/2$ at $1.5 \times 10^{-2} \text{ M}$ HClO_4 (min)
3-chlorophenol	6.5	34
2-chlorophenol	14.5	125
4-chlorophenol	12.5	> 180
3,4-dichlorophenol	6.3	16
2,4,5-trichlorophenol	12	36

Table 3, - Extraction Efficiency as a Function of Experimental
Parameters for Iron(III)-PAS-C₇

pH	% E	PAS-C ₇ , M	% E	Triton X100/ BL 4.2, % w/v	% E
2.00	39.0	5×10^{-4}	80.0	0.50:0.50	77.6
2.65	74.5	1×10^{-3}	87.5	0.75:0.75	93.6
3.10	88.4	1.5×10^{-3}	92.0	1.00:1.00	93.7
3.50	93.7	2×10^{-3}	93.7	1.50:1.50	94.0
3.75	94.3				

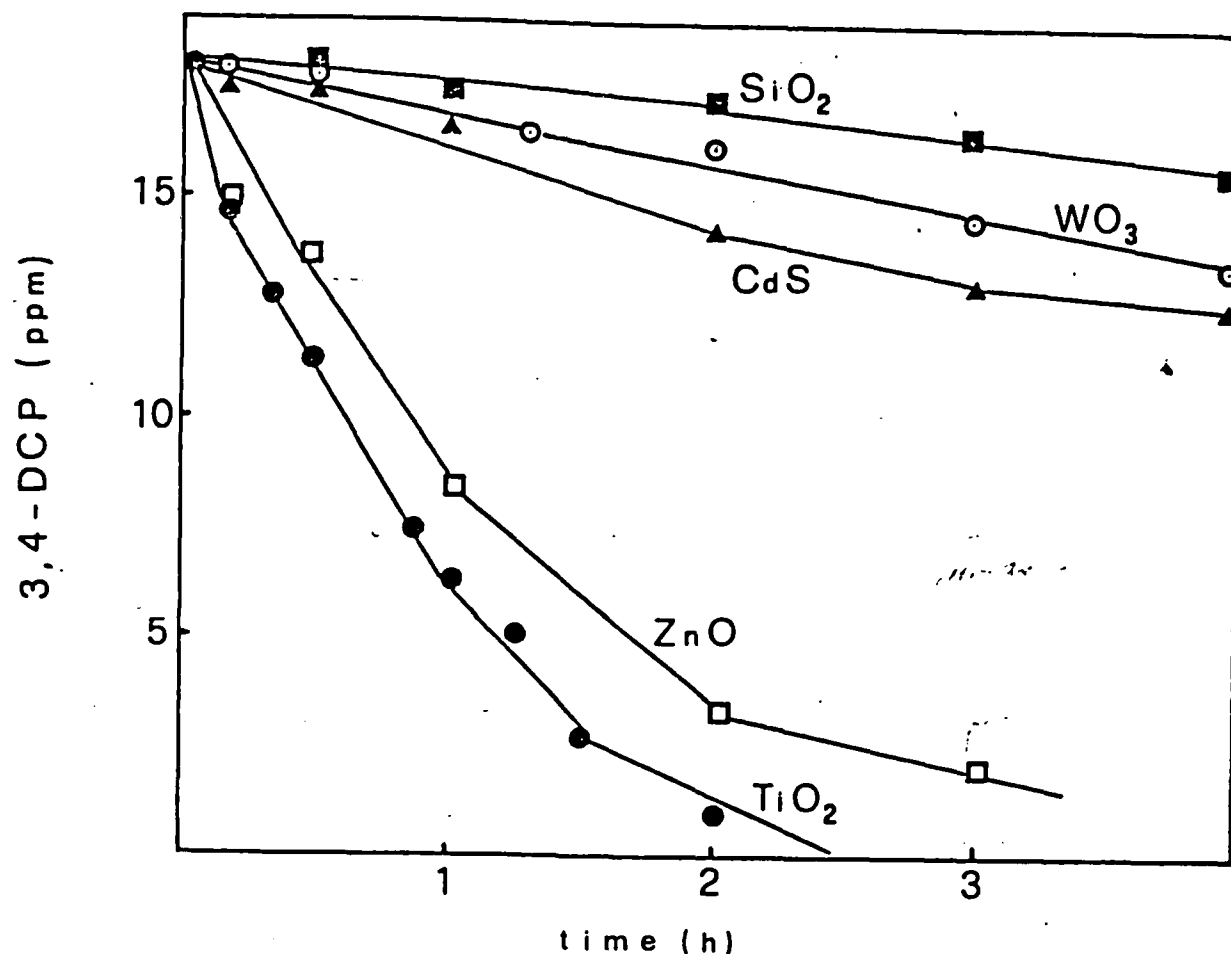


Figure 1. Photodegradation of 3,4-dichlorophenol in the presence of various semiconductor dispersions; wavelength of irradiation > 330 nm; initial 3,4-DCP concentration 18 ppm; O₂ present; initial pH 3.0; unbuffered aqueous solutions; concentration of catalyst, 2.0 g/l.

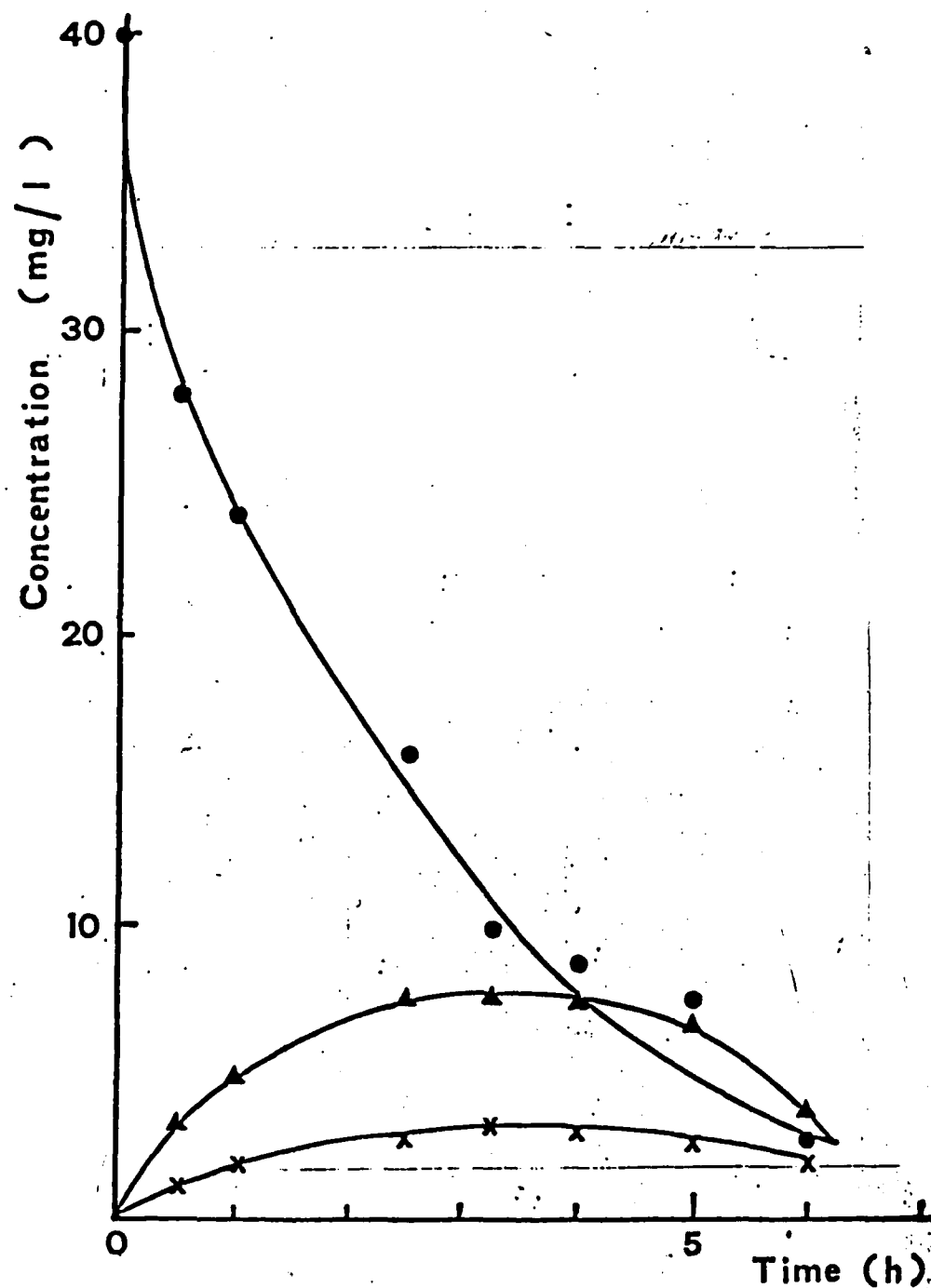


Figure 2 Results of phenol degradation and intermediate formation in the presence of TiO_2 (2 g/l); phenol concentration 40 mg/l; Xenon lamp power 150 W; (●) phenol; (X) quinol; (▲) catechol

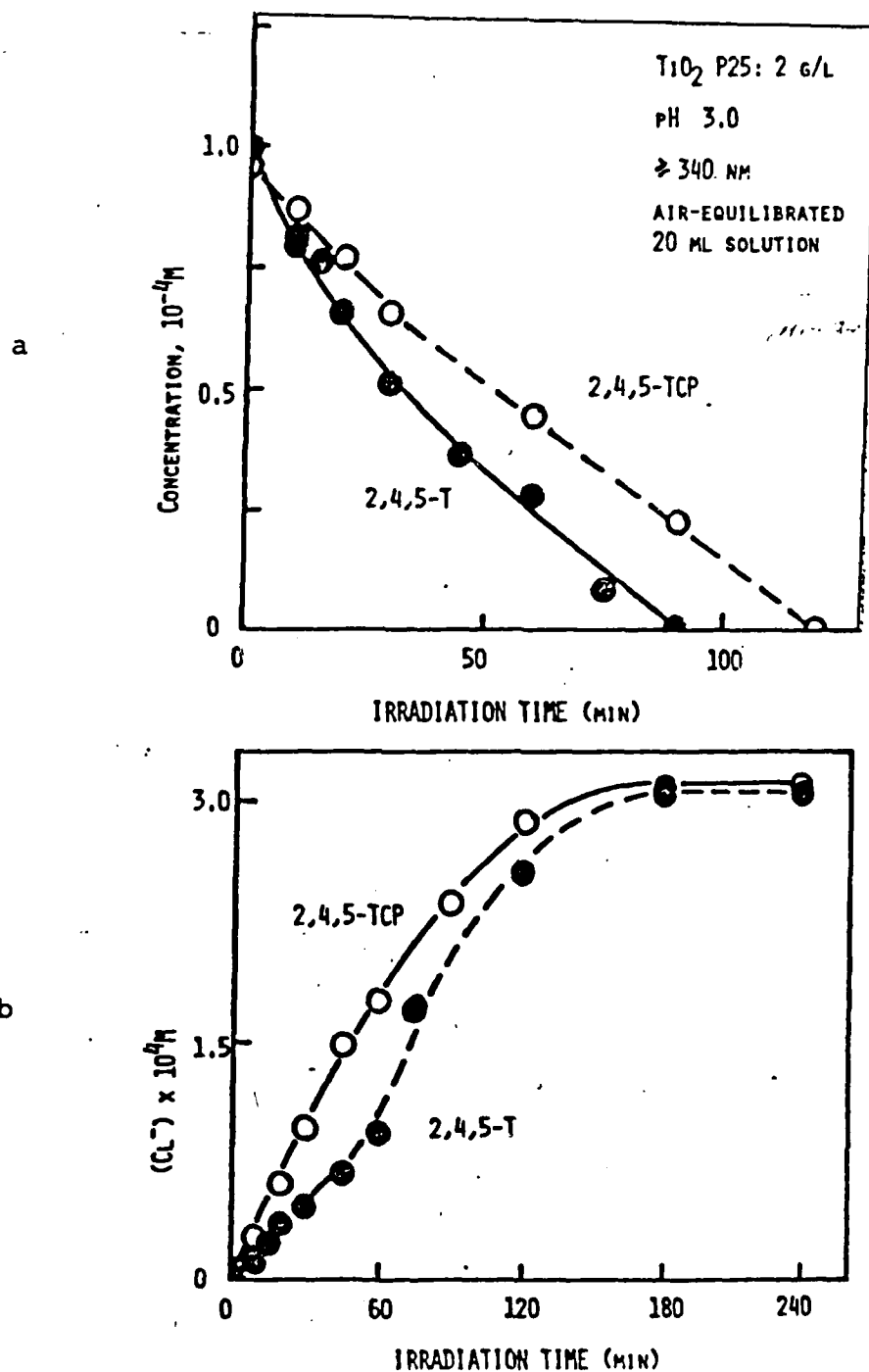


Figure 3 (a) Plot showing the relative decomposition of 2,4,5-T and 2,4,5-TCP as a function of irradiation time
 (b) Plot showing the formation of stoichiometric quantities of chloride ions as a function of irradiation time

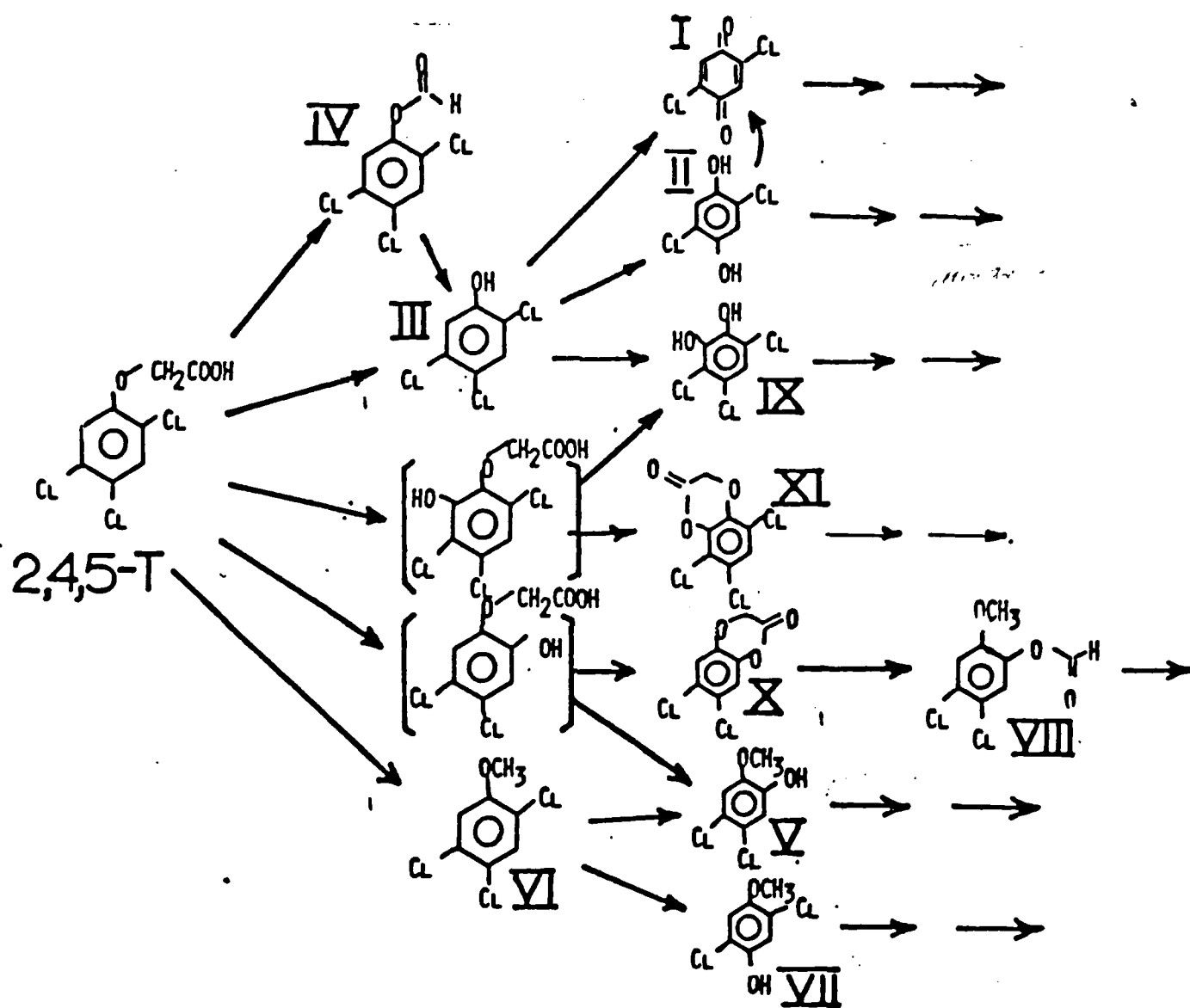
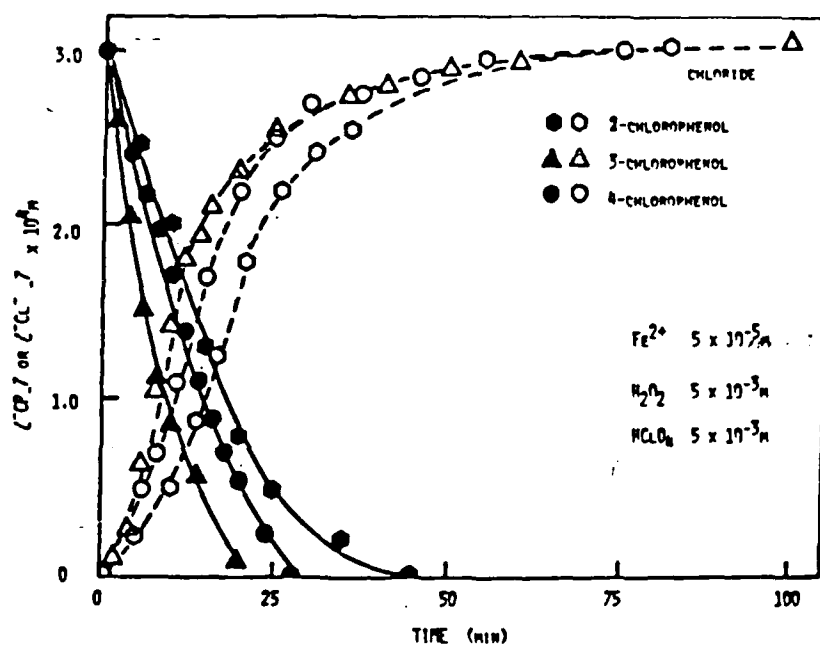


Figure 4 Plausible photodegradation pathway of 2,4,5-T in the presence of TiO_2 under simulated sunlight irradiation conditions.

5



6

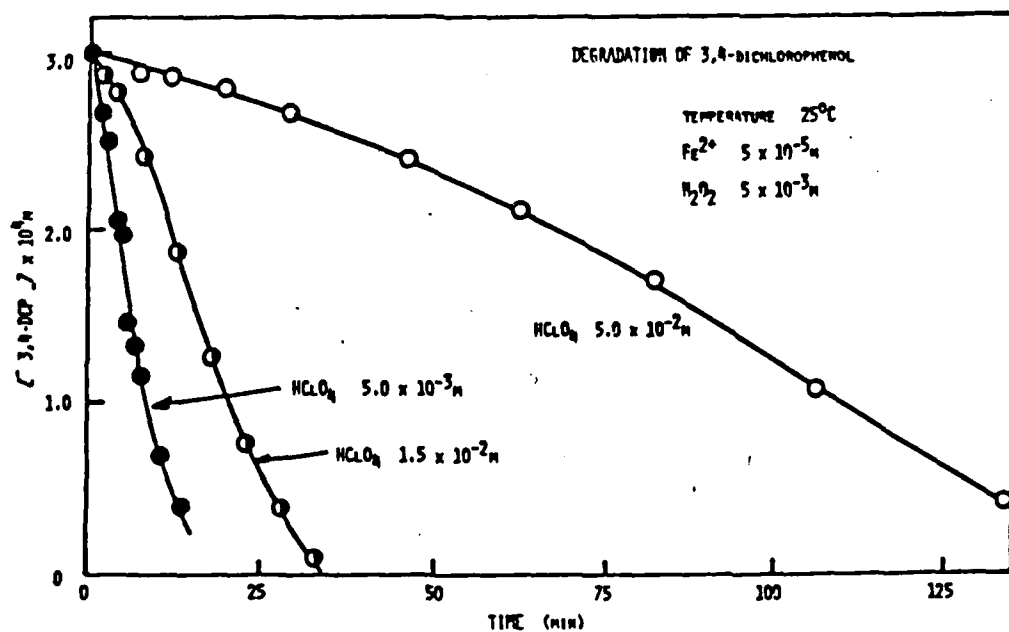


Figure 5 Degradation of monochlorophenols by Fenton's reagent and concomitant appearance of free chloride ions.

Figure 6 Disappearance of 3,4-DCP as a function of time at different HClO_4 concentrations.

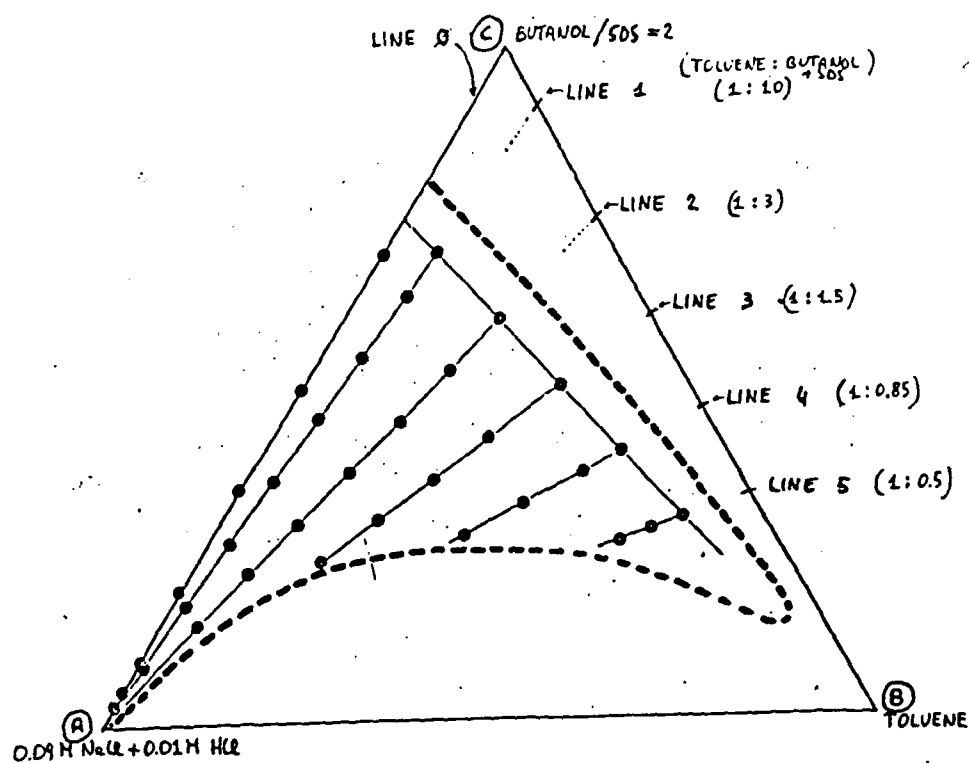


Figure 7 Pseudoternary phase diagram of the system water (0.09 M NaCl + 0.01 M HCl) - toluene - (1-butanol:SDS = 2:1), showing the single-phase at 25 C. The straight lines represent the dilution lines by water and the points the microemulsion compositions at which the kinetic runs were performed

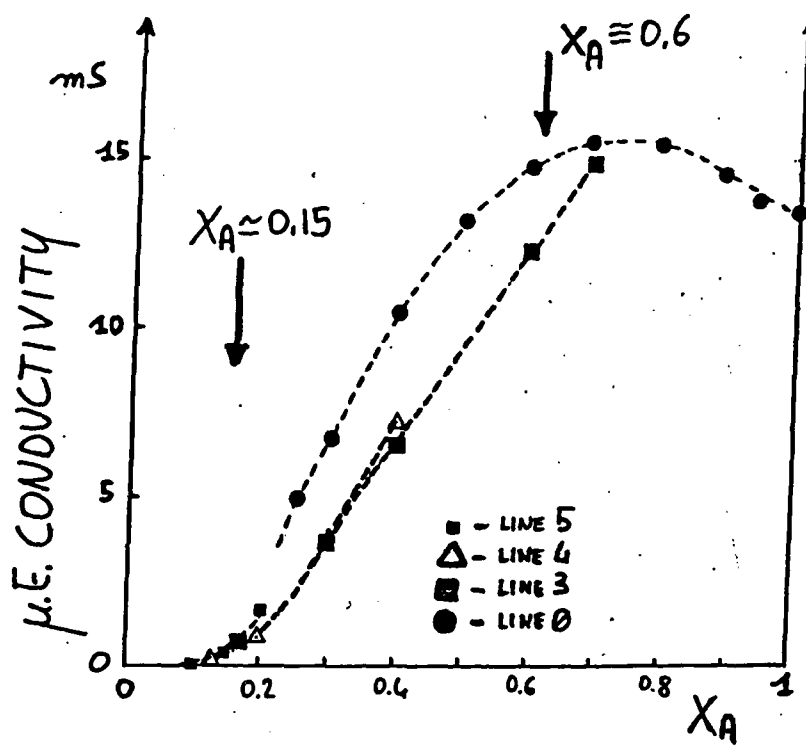


Figure 8 Conductance of a series of microemulsions, according to the lines shown in Fig. 7

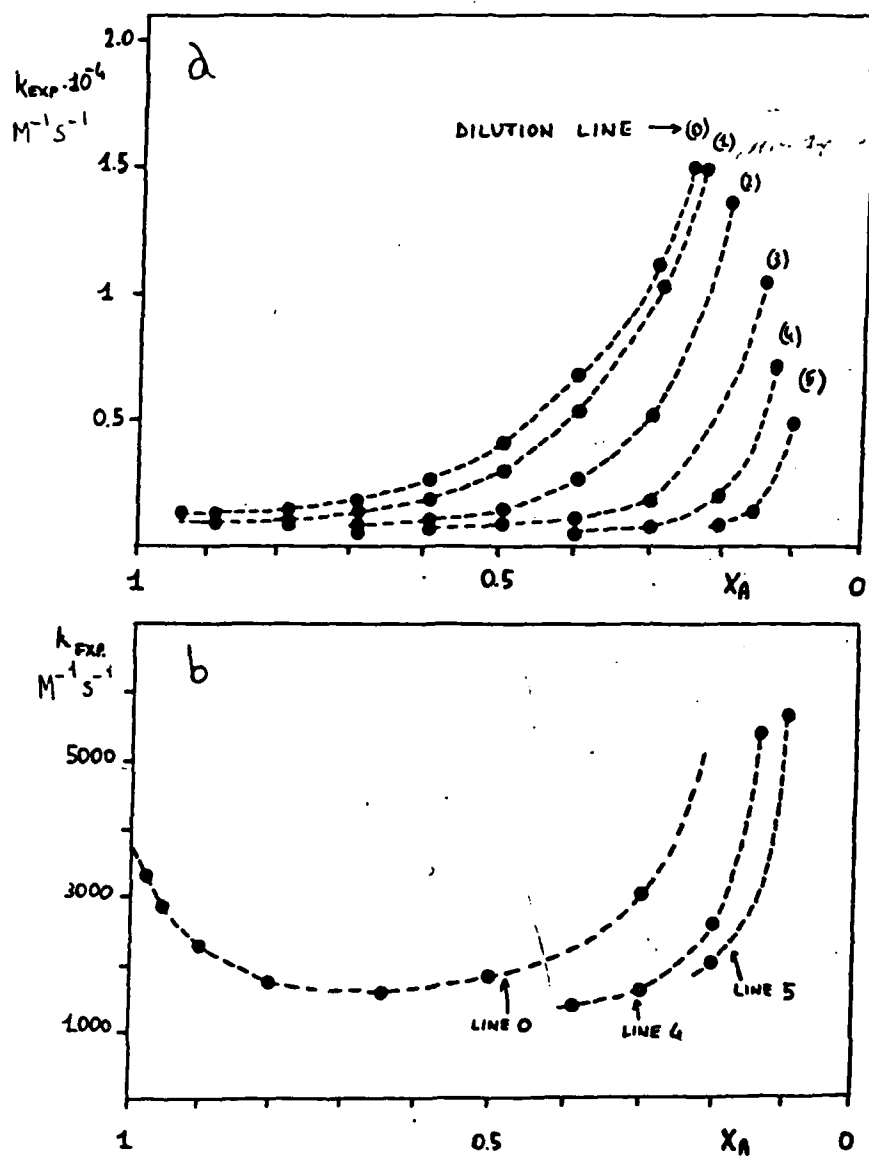


Figure 9 Experimental rate constants for the oxidation of catechols by IrCl_6^{2-} in microemulsions (for the dilution lines see Fig. 7)
 (a) di-t-butylcatechol (b) catechol

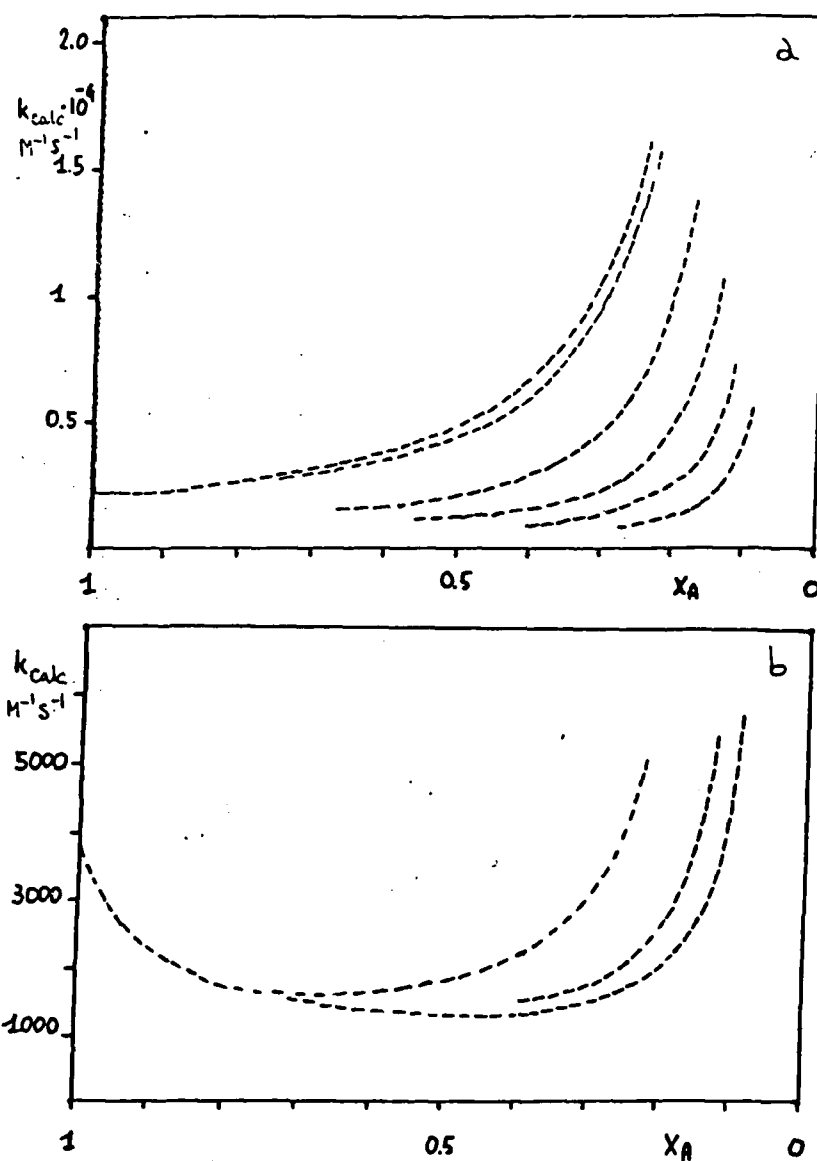


Figure 10 Calculated rate constants according eq. (24) - (26).
 (a) di-t-butylcatechol (b) catechol

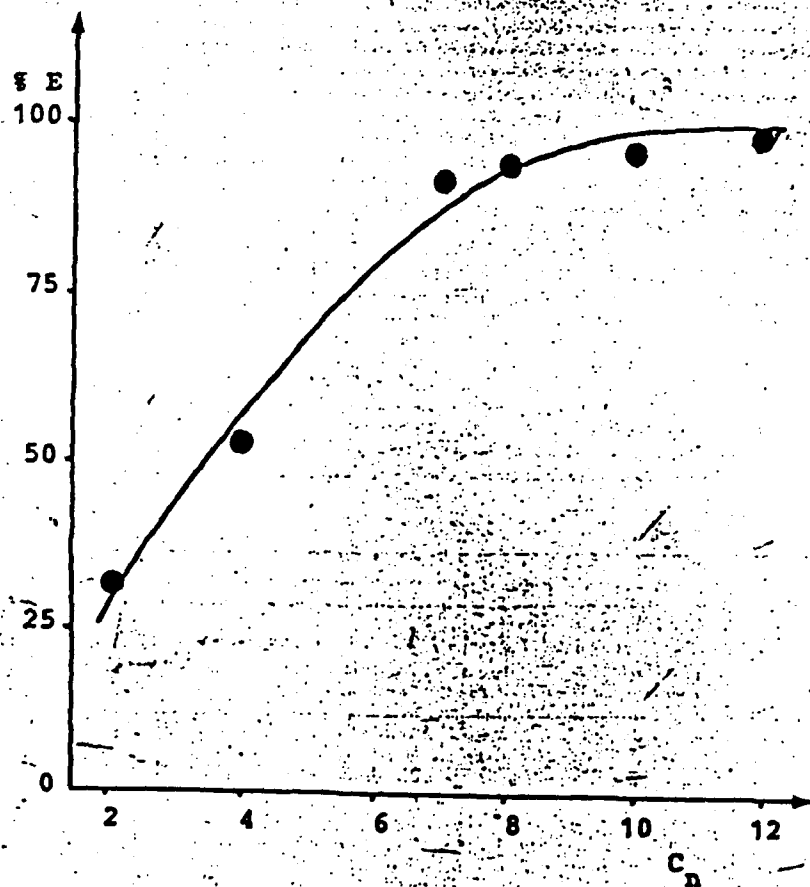


Figure 11 Plot of the percent extraction of iron (III) as a function of ligand alkyl chain length.

END

DATE

FILMED

8-88

DTIC